

The Effect of Temperature on the Corrosion Inhibition of Mild Steel in 1 M HCl Solution by *Curcuma Longa* Extract

Nurul Izni Kairi*, Jain Kassim

Materials and Corrosion Chemistry Laboratory, School of Chemical Sciences, Universiti Sains Malaysia, 11800 Penang, Malaysia.

*E-mail: iznikairi@gmail.com

Received: 20 December 2012 / Accepted: 9 April 2013 / Published: 1 May 2013

The corrosion inhibition mechanism of the *Curcuma longa* extract on mild steel surface in 1 M HCl has been studied at different temperatures (30-55 °C) by gravimetric measurements. The inhibition efficiency decreases with increasing temperature. As the concentration of the extract increased, higher activation energy, enthalpy of activation and entropy of activation were obtained. The inhibition were physisorption in nature with an endothermic reaction. The adsorption process was more favoured at lower temperatures with larger negative standard free energy. The adsorption process on the mild steel surface obeys the Langmuir adsorption isotherm.

Keywords: organic compounds; electron microscopy; corrosion; adsorption; thermodynamic properties; surface properties.

1. INTRODUCTION

Corrosion is a natural occurring process where it can be defined as the deterioration of a material's properties due to its interaction with its environment. Corrosion can lead to failures in plant infrastructure and machines which are usually costly to repair, in terms of loss of contaminated products, environmental damage and possibly costly in terms of human health. The driving force that causes metals to corrode is due to the natural consequence of their temporary existence in metallic form. The primary corrosion product of iron, exists as, eg. $\text{Fe}(\text{OH})_2$, or more likely $\text{FeO}\cdot\text{nH}_2\text{O}$, but the action of oxygen and water can yield other products having different colours [1]:

- $\text{Fe}_2\text{O}_3\cdot\text{H}_2\text{O}$ or hydrous ferrous hydroxide, sometimes written as $\text{Fe}(\text{OH})_3$, is the principle component of red-brown rust. It can form a mineral called hematite which is the most common iron ore.

- $\text{Fe}_3\text{O}_4 \cdot \text{H}_2\text{O}$ or hydrated magnetite, known as ferrous ferrite, written as $(\text{Fe}_2\text{O}_3 \cdot \text{FeO})$, most often green but can be deep blue in the presence of organic complexants.
- Fe_3O_4 or magnetite which is black.

Mild steel being the important alloy of iron has found a wide application in industries, constructional materials and machines due to its low cost and excellent mechanical properties despite of its tendency to corrosion in aqueous solution, especially in acidic media [2-5]. Acid solutions are often used in the industry for industrial acid cleaning, pickling, descaling, oil well acidizing and petrochemical processes which are normally accompanied by considerable dissolution of metal [6-10]. The use of corrosion inhibitor is usually the most promising, effective, flexible and cost attractive method to reduce the corrosive attack of acid solutions [11, 12]. Corrosion inhibitors are chemical compound usually used in small concentration which when added to a corrosive media retards the corrosion process and keeps its rate to a minimum [13, 14]. Among them, organic compounds containing heteroatoms such as nitrogen, oxygen, sulphur and phosphorus, π electrons in triple or conjugated double bonds possess the ability to act as good corrosion inhibitor as they are easily adsorbed onto the metal surface [15-19]. It is widely accepted that organic inhibitors exhibit corrosion via adsorption. The inhibition mechanism is a separation process involving (i) the inhibitor is adsorbed on the surface of the metal forming a compact protective thin layer and (ii) the inhibitor forms a precipitate on the surface of the metal, acting on the aggressive media to form protective precipitates or remove the aggressive agents [20]. Adsorption, on the other important notes can be described by two main types of interaction, which are physisorption and chemisorption, where [21, 22]:

- *Physisorption*: involves electrostatic forces between ionic charges or dipoles on the adsorbed species and the electric charge at the metal/solution interface. The heat of adsorption is low, thus, this adsorption is only stable at relatively low temperature.
- *Chemisorption*: involves charge transfer or sharing from the inhibitor molecules to the metal surface to form a coordinate type bond. This type of adsorption is known to have much stronger adsorption energy compared to the other mode of adsorption. Thus, such bond is more stable at higher temperature.

Unfortunately, most of the reported inhibitors used in the industry are highly toxic, so they are very hazardous to the environment, expensive and non-environmentally friendly, thus these factors limit their applications [23, 24]. Many environmental laws have been made to impose and to divert researchers to the use of natural products as an alternative substitution. The employment of natural products extracted from leaves, rhizomes, seeds or bark of the extracts are due to its 'green' effects, practical use, inexpensive, relatively non-toxic, readily available and comes from renewable resources.

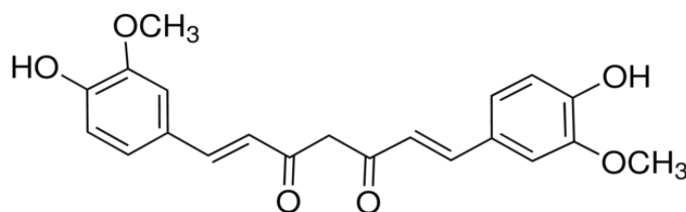


Figure 1. Chemical structure of curcumin.

Curcuma longa or generally known as turmeric has long been used as a common household medicine, food colorant and spice in Southeast Asia. It is known that curcumin; 1,7-bis(4-Hydroxy-3-methoxyphenyl)-1,6-heptadiene-3,5-dione (Fig. 1) is the major active compound found in turmeric.

The other two curcuminoids are demethoxy curcumin (Fig. 2) and bis-demethoxy curcumin (Fig. 3). These three curcuminoids are natural phenol and they are responsible for the yellow colour of turmeric. The structural of these curcuminoids itself which possess heterocyclic compounds with polar functional group, conjugated double bonds, hydroxyl, oxygen and the non-toxicity factors that show the ability to act as organic corrosion inhibitor, there comes our interests to choose turmeric extracts to be used as corrosion inhibitor.

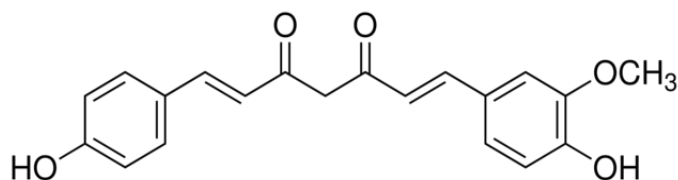


Figure 2. Chemical structure of demethoxy curcumin.

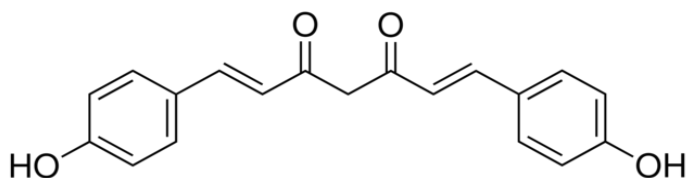


Figure 3. Chemical structure of bis-demethoxy curcumin.

Thermodynamic adsorption parameters and kinetics of corrosion parameters are useful for clarifying the adsorption behaviour of an inhibitor [21]. The effect of temperature on the inhibited acid-metal reaction is highly complex because many changes occur on the metal surface, such as rapid etching, desorption of inhibitor and the inhibitor itself may undergo decomposition and/or rearrangement [21, 26]. The aim of this work is to investigate the inhibition, pH and temperature effects of turmeric extracts, hence to study the thermodynamic of adsorption and activation energies of the extract in order to clarify how this inhibitor works on mild steel in 1 M HCl by using gravimetric measurements.

2. EXPERIMENTAL

2.1 Preparation of extract

Raw materials of fresh *Curcuma longa* rhizomes were purchased from a local supermarket in Malaysia as the starting material. The rhizomes were cleaned, cut into smaller pieces and ground into

powder (~250 mesh) followed by further drying at 50 °C to a constant weight. The dried rhizome powder of turmeric was defatted twice overnight using 25 mL hexane (1:5 m/v) at 200 rpm at room temperature (30 ± 2 °C) by means of maceration technique for the removal of lipid and oils from the extract. The defatted residue was then extracted with 95% aqueous ethanol (1:10 m/v) incubated for 3 hours by means of orbital shaker at 200 rpm. Afterwards, the extract was concentrated at 50 °C under reduced pressure by means of rotary evaporator to remove the ethanol. The aqueous fraction was then freeze dried to remove the water content.

2.2 Preparation of metal specimen

The mild steel specimens having composition (wt%) of 0.14% C, 0.20% Si, 0.15% Mn, 0.10% Ni, 0.14% Cu and remaining Fe were mechanically abraded with a series of emery papers from 120 to 1200 grades. The samples were then washed thoroughly with distilled water, degreased with isopropanol and air dried.

2.3 Preparation of test solution

The test solutions were prepared by the dilution of analytical grade 37% HCl with distilled water up to the optimum inhibitor concentration of the extract. For pH studies, the test solutions were prepared by the dilution of distilled water up to the optimum concentration where it can reach by adjusting the pH using HCl and NaOH. Inhibitors were dissolved in acid solution at required concentrations in ppm (mg L^{-1}) and the solution in the absence of inhibitor was taken as blank for comparison purposes. Due to the fact that curcumin which is the major active compound in turmeric has low aqueous solubility, hence both of the test solutions were first dissolved in 10% ethanol and they were put in sonicator for 5 minutes.

2.4 Determination of total phenolic content

The total phenolic content (TPC) in the extract and standard curcumin were determined by using the method described by Tan et al., (2010) [27]. 5.0 mL (1/10 dilution) of the Folin-Ciocalteu reagent was dissolved in a test tube containing 0.5 mL diluted extract or standard solution of gallic acid (20, 40, 60, 80 and 100 ppm). The solution was kept at room temperature for 5 minutes. After that, 4 mL of 1 M sodium carbonate (Na_2CO_3) was added and the solution was diluted to 10.0 mL and the final mixture was mixed thoroughly. After 2 hours of incubation in the dark at room temperature, the absorbance value versus blank was measured at 760 nm. Total phenolic content of the sample was expressed as gallic acid equivalent concentration (mg of GAE/ g dry sample) through the calibration curve of gallic acid. Samples were analyzed in duplicate to obtain good reproducibility. Standard curcumin (C1386) of ~70% purity from Sigma-Aldrich was used for reference purposes.

2.5 Gravimetric study

The gravimetric method (weight loss, w_L) is known to be the most widely used method of monitoring inhibition efficiency [18]. The mild steel specimens of dimension 4 x 3 x 0.1 cm were used in these studies. The weight loss measurements were conducted under total immersion using 250 mL capacity beakers containing 100 mL of test solutions with and without the extract for 24 hours at 30, 35, 45 and 55 °C (303 K, 308 K, 318 K and 328 K) maintained in a thermostated water bath. The specimens were weighed before and after the tests using an analytical balance with a precision of 0.1 mg. The specimens were taken out after the 24 hours of immersion, washed, dried and reweighed accurately to determine the weight loss of mild steel. For pH studies, same method have been applied, except the pH of the test solutions were first been adjusted to the desired pH. All measurements were performed few times and average values were reported to obtain good reproducibility. The corrosion rate (ρ) in $\text{mg cm}^{-2} \text{h}^{-1}$ in the absence and presence of extract was determined using the following equation:

$$\rho = \frac{\Delta W}{At} \quad (1)$$

where ΔW is the average weight loss of the mild steel specimens, A is the total area of mild steel specimen and t is the immersion time in 24 hours. The percentage inhibition efficiency (IE%) was calculated using the relationship:

$$IE\% = \frac{W_o - W_i}{W_o} \times 100 \quad (2)$$

where W_o and W_i are the weight loss values in the absence and presence of extract.

2.6 SEM-EDX analysis

The surface morphology of the corroded and inhibited species of mild steel was investigated by using scanning electron microscopy (LEO Supra 50 VP Field Emission SEM) equipped with Oxford INCA x activation energy dispersive x-ray microanalysis system (Carl-Ziess SMT). The images were taken after immersing the samples for 24 hours at room temperature in 1 M HCl without and with the presence of 60 ppm and 80 ppm of the extract.

3. RESULTS AND DISCUSSION

3.1 Total phenolic content

Total phenolic content as summarized in Table 1 were quantified based on the linear equation of gallic acid standard calibration curve. Comparison of total phenolic content between the extract and

standard curcumin clearly proved that the extract gives 97.13 mg GAE/ g dry sample while standard curcumin gives 184.63 mg GAE/ g dry sample. The theory of Folin-Ciocalteu assay lies on the reduction of a phosphotungstate-phosphomolybdate complex by phenolics to a mixture of blue oxides which have a maximal absorption in the region of 760 nm [28]. In conjunction with the extract and standard curcumin, after the addition of Folin-Ciocalteu reagent to the samples, the yellow colour of the reagent will be converted into blue colour solution as an indication that there is phenolic content present in the extract as in the standard curcumin.

Table 1. The effect of different samples on phenolic profile.

Sample(s)	TPC (mg GAE/g dry sample)
Extract	97.13 ± 3.01
Standard curcumin	184.63 ± 3.01

Data are expressed as mean ± standard deviation (n=2)^a.

3.2 Gravimetric study

3.2.1 Effect of pH

Table 2. Inhibition efficiency for various pH of 80 ppm extract at 30 °C for the corrosion of mild steel.

pH	0	1	2	3	4	5	6	7
IE (%)	79.81	47.59	40.88	37.50	28.57	20.64	16.67	9.09

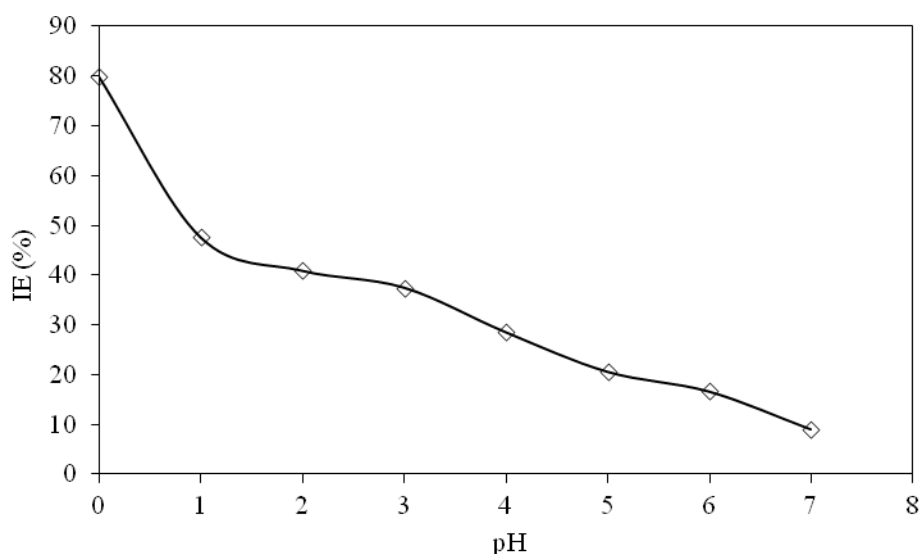


Figure 4. Effect of pH on inhibitor performance.

The influence of pH on the corrosion of mild steel has been studied in the range of pH 1-7 of 80 ppm extract at room temperature (30 °C). This study is important to gain knowledge concerning the efficiency of the extract at various pH to which the addition of the extract will give highest inhibition, and to which the mild steel is seriously corroded. Fig. 4 and Table 2 show the results on the effect of pH.

As pH values approaching 0, which is the pH values in 1 M HCl media, the inhibition efficiency is at its maximum. It is remark from the results that the corrosiveness of acid is the main factor contributing to the aggressive attack on the mild steel surface, thus leading to the highest inhibitory effect of the extract. The corrosion parameters obtained by conducting the weight loss study at pH 5, which is the pH at which the extract is being prepared in distilled water media are presented in Fig. 5.

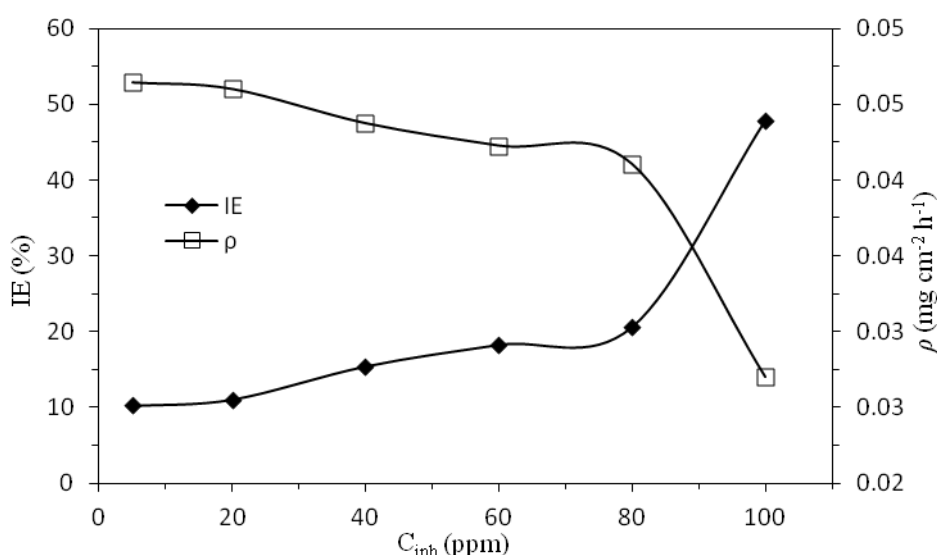


Figure 5. Relationship between corrosion rate (ρ) and the inhibition efficiency (IE) with the concentration of extract for mild steel in 1 M HCl after 24 hours at pH 5.

It is apparent that the inhibition efficiency increases with increasing concentration and the corrosion rate decreases as the concentration of the extract increases. However, due to the fact that mild steel is mildly corroded at pH near neutral and the corrosive attack of mild steel in 1 M HCl at pH 0 is severe, the studies on 1 M HCl is in our main scope of interests.

3.2.2 Effect of temperature

The corrosion parameters obtained by conducting weight loss measurements for mild steel in the absence and presence of different concentration of extract in 1 M HCl at different temperature are tabulated in Table 3. It can be clearly seen that the corrosion rate values decreased and inhibition efficiency increased with the increase in the concentration of extract. This might be due to the fact that the adsorption coverage of the inhibitor on mild steel surface increases with the concentration of the

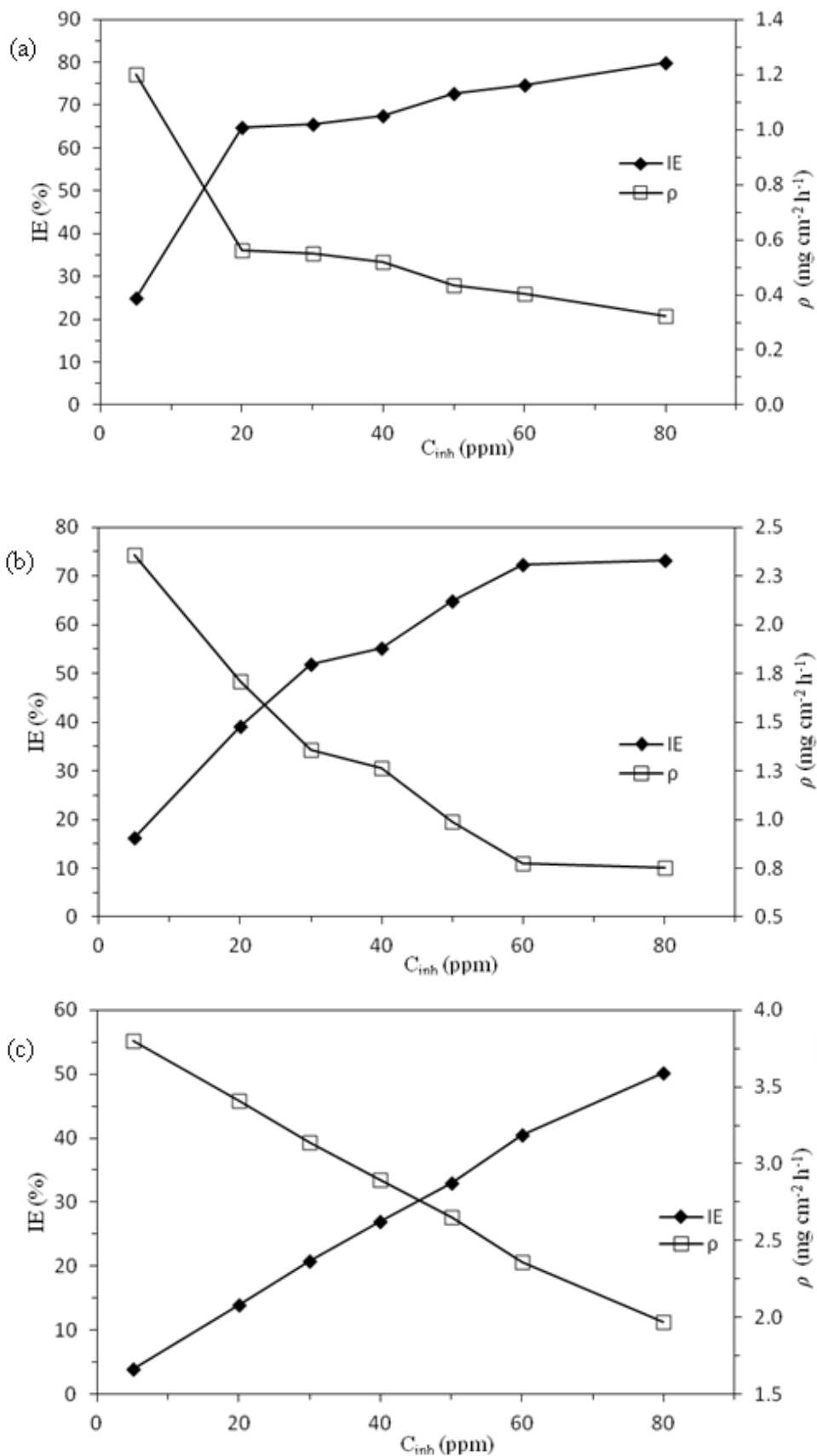
extract. The variation of corrosion rate and inhibition efficiency with concentration of the extract are shown in Figs. 6 (a, b, c and d). It can be observed that the corrosion rate of mild steel decreases while the inhibition efficiency increases as the concentration of the extract increases.

Table 3. Corrosion parameters for mild steel in 1 M HCl containing various concentrations of extract at the influence of temperature.

T (K)	C_{inh} (ppm)	w_L (mg)	ρ ($\text{mg cm}^{-2} \text{h}^{-1}$)	IE (%)	Θ
303 K	Blank	921.30	1.60	-	-
	5	690.95	1.20	25.00	0.2500
	20	323.85	0.56	64.85	0.6485
	30	316.51	0.55	65.65	0.6565
	40	298.35	0.52	67.62	0.6762
	50	251.15	0.44	72.74	0.7274
	60	232.80	0.40	74.73	0.7473
	80	186.00	0.32	79.81	0.7981
	308 K	Blank	1621.50	2.82	-
5		1358.30	2.36	16.23	0.1623
20		986.00	1.71	39.19	0.3919
30		780.40	1.35	51.87	0.5187
40		726.90	1.26	55.17	0.5517
50		569.45	0.99	64.88	0.6488
60		447.20	0.78	72.42	0.7242
80		432.80	0.75	73.31	0.7331
318 K		Blank	2280.90	3.96	-
	5	2189.40	3.80	4.01	0.0401
	20	1962.60	3.41	13.96	0.1396
	30	1807.74	3.14	20.74	0.2074
	40	1666.00	2.89	26.96	0.2696
	50	1527.50	2.65	33.03	0.3303
	60	1357.90	2.36	40.47	0.4047
	80	1137.20	1.97	50.14	0.5014
	328 K	Blank	2698.30	4.68	-
5		2671.60	4.64	0.99	0.0099
20		2606.80	4.53	3.39	0.0339
30		2561.20	4.45	5.08	0.0508
40		2534.90	4.40	6.06	0.0606
50		2502.10	4.34	7.27	0.0727
60		2453.60	4.26	9.07	0.0907
80		2387.40	4.14	11.52	0.1152

It is noted that the inhibition efficiency depends on temperature and decreases with the rise of temperature, indicating that at higher temperature, dissolution of mild steel predominates on the

surface. This effect can be explained by the decrease of the strength of the adsorption process at high temperature, suggesting physical adsorption [29].



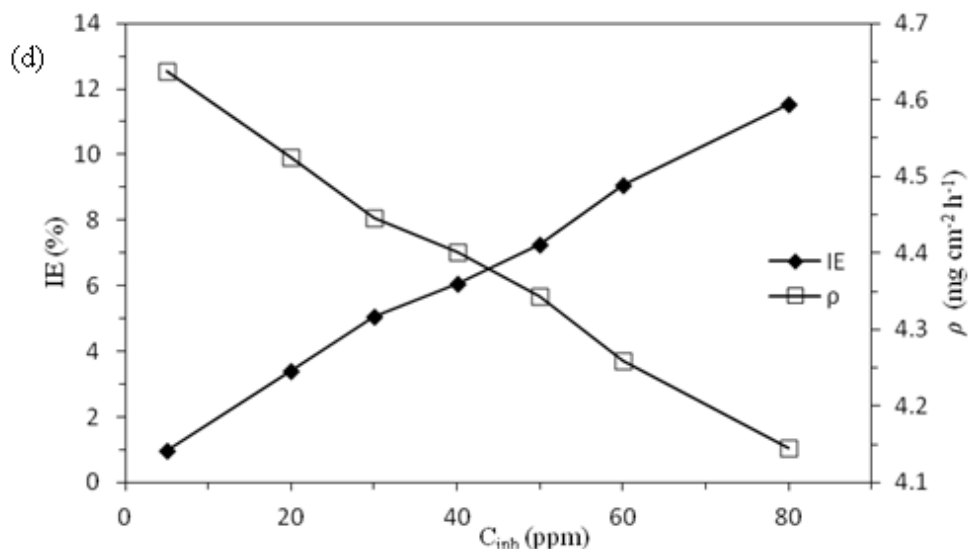


Figure 6. Relationship between corrosion rate (ρ) and the inhibition efficiency (IE) with the concentration of extract for mild steel in 1 M HCl after 24 hours at different temperature: (a) 303 K, (b) 308 K, (c) 318 K and (d) 328 K.

The increase in temperature might stimulate larger metal surface kinetic energy, which has an adverse effect on the adsorption process where it weakens the adsorption process and encourage desorption process, hence the equilibrium shift towards desorption as follows [30]:



3.2.3 Corrosion kinetic parameters

The dependence of the corrosion rate on temperature can be expressed by the Arrhenius equation and transition state equation as presented in Eqs. (4) and (5), respectively [29-33]:

$$\log \rho = \frac{-E_a}{2.303 RT} + \log A \tag{4}$$

$$\rho = \frac{RT}{Nh} \exp \frac{\Delta S}{R} \exp \frac{-\Delta H}{RT} \tag{5}$$

where ρ is the corrosion rate, E_a is the apparent activation energy, R is the universal gas constant ($8.314\ J\ mol^{-1}\ K^{-1}$), T is temperature, A is the Arrhenius pre-exponential factor, h is the Plank's constant ($6.626176 \times 10^{34}\ J\ s$), N is the Avogadro's number ($6.02252 \times 10^{23}\ mol^{-1}$), ΔS is the entropy of activation and ΔH is the enthalpy of activation. The plot of $\log \rho$ against $1/T$ is presented in Fig. 7. The slope of the line is $(-E_a/2.303 RT)$ and the intercept of the line extrapolated gives $\log A$. Analysis of the temperature dependence on inhibition efficiency as well as comparison of corrosion activation energy in the absence and presence of inhibitors give an insight knowledge on the possible mechanism of inhibitor adsorption. A decrease in inhibition efficiency with rise in temperature with an

increase in E_a in presence of inhibitor compared to the absence, is frequently being interpreted as the formation of an adsorptive film of physisorption [34].

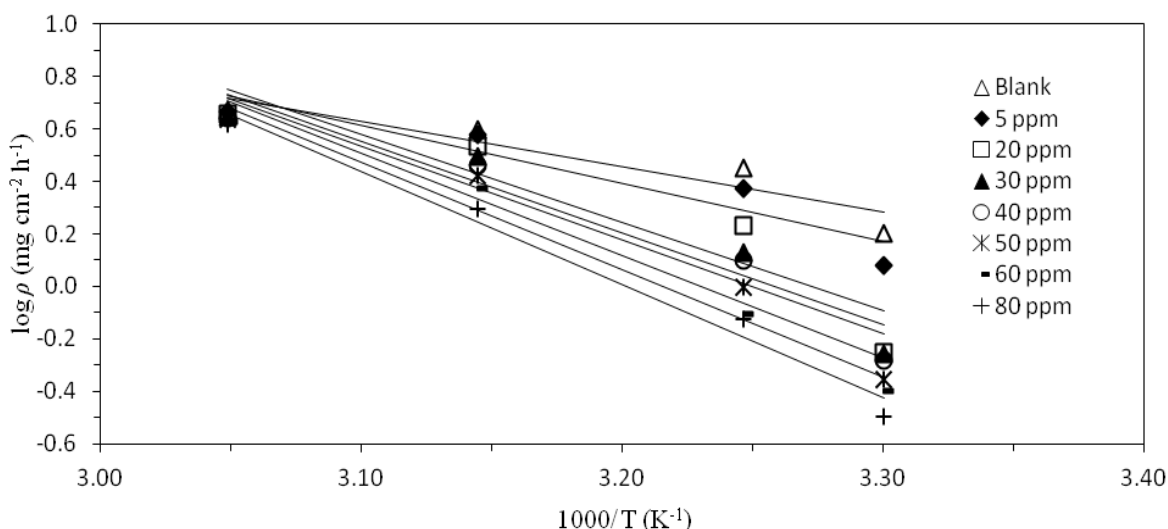


Figure 7. Arrhenius plots for mild steel corrosion in 1 M HCl in the absence and presence of different concentrations of extract.

All calculated parameters are given in Table 4. Higher values of E_a in the presence of extract which acts as inhibitor is a good indication of strong inhibitive action of the extract by increasing the energy barrier for the corrosion process. Higher values of E_a in the presence of extract can also be correlated with the increase in thickness of the double layer that enhance the E_a of the corrosion process [35].

Table 4. Activation parameters, pre-exponential factor, enthalpy and entropy of dissolution reaction of mild steel in 1 M HCl containing various concentrations of extract.

Media (ppm)	A (mg cm ⁻² h ⁻¹)	E_a (kJ mol ⁻¹)	r^2	ΔH (kJ mol ⁻¹)	ΔS (J mol ⁻¹ K ⁻¹)	r^2
Blank	9.40 x 10 ⁵	33.02	0.8731	30.40	-139.39	0.8531
5	2.81 x 10 ⁷	42.22	0.8864	39.60	-111.15	0.8725
20	1.06 x 10 ¹¹	64.51	0.8646	61.89	-42.67	0.8544
30	2.45 x 10 ¹¹	66.94	0.9235	64.32	-35.69	0.9174
40	3.81 x 10 ¹¹	68.23	0.9375	65.61	-32.01	0.9326
50	3.90 x 10 ¹²	74.64	0.9603	72.02	-12.67	0.9573
60	1.67 x 10 ¹³	78.75	0.9804	76.13	-10.63	0.9789
80	6.32 x 10 ¹³	82.52	0.9805	79.90	10.49	0.9791

Fig. 8 shows the plot of $\log \rho/T$ vs $1/T$. Straight line were obtained with the slope of $(\Delta H/2.303 RT)$ and an intercept of $[(\log (R/Nh) + (\Delta S/2.303 RT))]$ from which the values of ΔH and ΔS ,

respectively were calculated and also listed in Table 4. The positive values of ΔH reflect the endothermic nature of the mild steel dissolution process. The negative values of ΔS imply that the disorderness is increased on going from reactant to product. It is observed that the shift of ΔS to more positive values on increasing the concentration of the extract is the driving force that can overcome the barriers for the adsorption of inhibitor onto the mild steel surface.

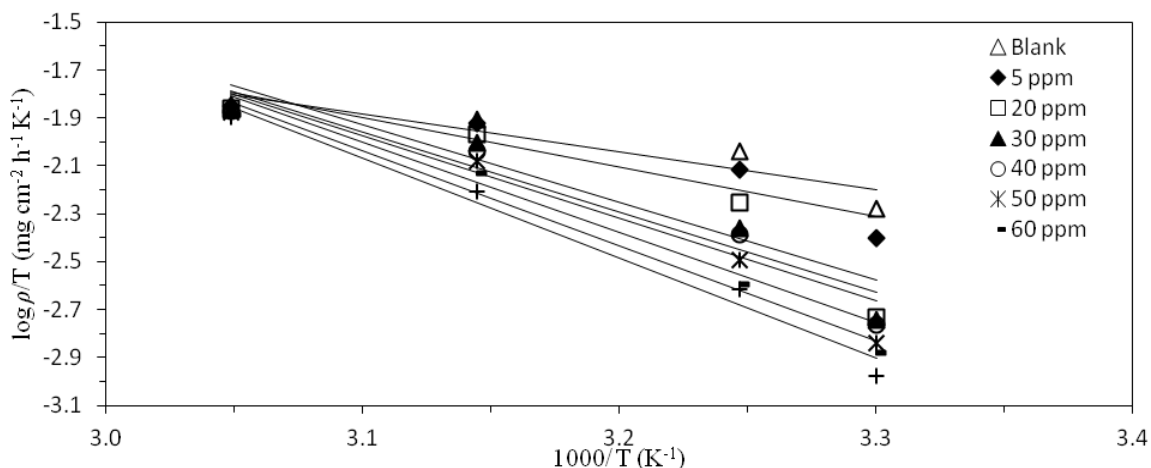


Figure 8. Transition state plots for mild steel corrosion in 1 M HCl in the absence and presence of different concentrations of extract.

3.2.4 Adsorption isotherm

It is useful to describe the adsorption process by an appropriate adsorption isotherm. The extent of corrosion inhibition mainly depends on the surface conditions and mode of adsorption of the inhibitor. Assumptions were made that the uncovered parts of the metal surface is equal to zero and the corrosion process takes place only at the uncovered parts of the metal surface. The degree of surface coverage (Θ) has been calculated as follows, $\Theta = IE/100$ by assuming a direct relationship between surface coverage and inhibition efficiency as presented in Table 3 [36]. In order to gain an insight to the mode of adsorption of the extract onto the mild steel surface, the surface coverage values were fitted into few adsorption isotherms and the values of correlation coefficient (r^2) were used to determine the best fit. The data were fitted to Langmuir, Frumkin, Temkin and Florry-Huggins adsorption isotherms according to the following equations [20, 37-45]:

$$\text{Langmuir: } \frac{C}{\Theta} = C + \frac{1}{K_{ads}} \quad (6)$$

$$\text{Frumkin: } \ln \left[\frac{\Theta}{(1-\Theta)C} \right] = \ln K_{ads} - 2a\Theta \quad (7)$$

$$\text{Temkin: } \Theta = \left(\frac{1}{f} \right) \ln(K_{ads} C) \quad (8)$$

$$\text{Florry-Huggins: } \log\left(\frac{\theta}{C}\right) = \log K_{ads} + x \log(1 - \theta) \tag{9}$$

where C is the concentration of extract, K_{ads} is the adsorptive equilibrium constant, f is the heterogenous factor of the metal surface describing the molecular interactions in the adsorption layer and the heterogeneity of the metal surface. If $f > 0$, mutual repulsion of molecules occur and if $f < 0$ attraction takes place. x is the number of inhibitor molecules occupying an active sites or the number of water molecules replaced by one molecule of the extract. K_{ads} is related to the standard free energy of adsorption, ΔG by the following equation [46-48]:

$$K_{ads} = \frac{1}{55.5} \exp\left(\frac{-\Delta G}{RT}\right) \tag{10}$$

where the numeral of 55.5 is the molar concentration of water in solution, R is the universal gas constant ($8.314 \text{ J mol}^{-1} \text{ K}^{-1}$) and T is temperature (K). The plots of C/θ versus C which is the Langmuir adsorption isotherm gives a straight line with an intercept of $1/K_{ads}$ as shown in Fig. 9. K_{ads} values are given in the unit of L mg^{-1} .

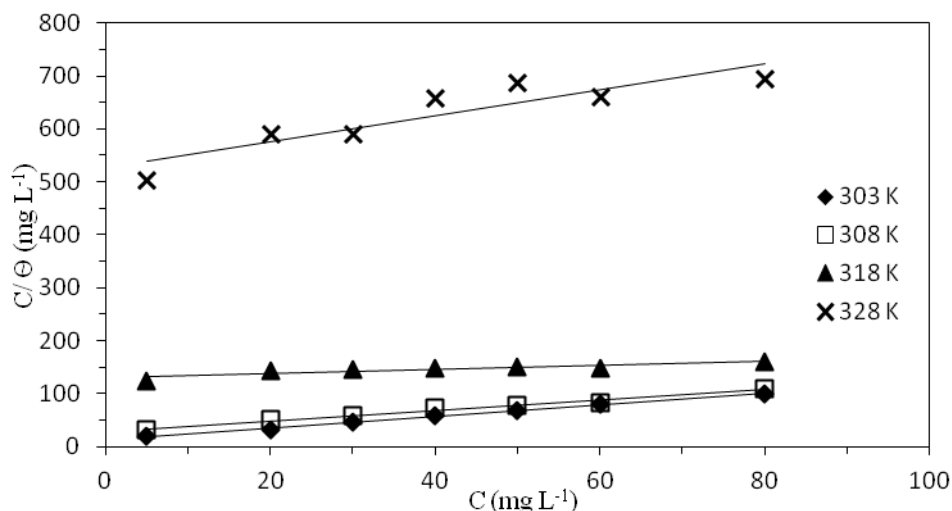


Figure 9. Langmuir adsorption isotherm plots at different temperatures.

Before calculating the parameters, the K_{ads} unit should be changed into L mol^{-1} (M^{-1}) in order to agree with the basic unit of SI and the calculated K_{ads} values in the unit of M^{-1} are given in Table 5, as well as various calculated parameters. Assumptions were made to account the molecular weight of the extract as $368.38 \text{ g mol}^{-1}$ as per the molecular weight of curcumin, which is the active compound in turmeric. Langmuir adsorption isotherm assumes that [49, 50]:

- (i) The metal surface contains a fixed number of adsorption sites and each site holds one adsorbate.
- (ii) ΔG is the same for all sites and it is independent of θ .

(iii) The adsorbates do not interact with one another, i.e. there is no effect of lateral interaction of the adsorbates on ΔG .

The linearity of the Langmuir plot may be interpreted to suggest that the experimental data obeyed the Langmuir adsorption isotherm. The negative values of ΔG suggests that the adsorption of inhibitors on mild steel surface is a spontaneous process. Generally, the adsorption type is regarded as physisorption if the values of up to -20 kJ mol^{-1} or lower, while those more negative than -40 kJ mol^{-1} involve sharing or transfer of electrons from the inhibitor molecules to the metal surface to form a coordinate type of bond, regarded as chemisorption [51-53]. High value of K_{ads} at lower temperature reflects the high adsorption ability of the extract on mild steel surface.

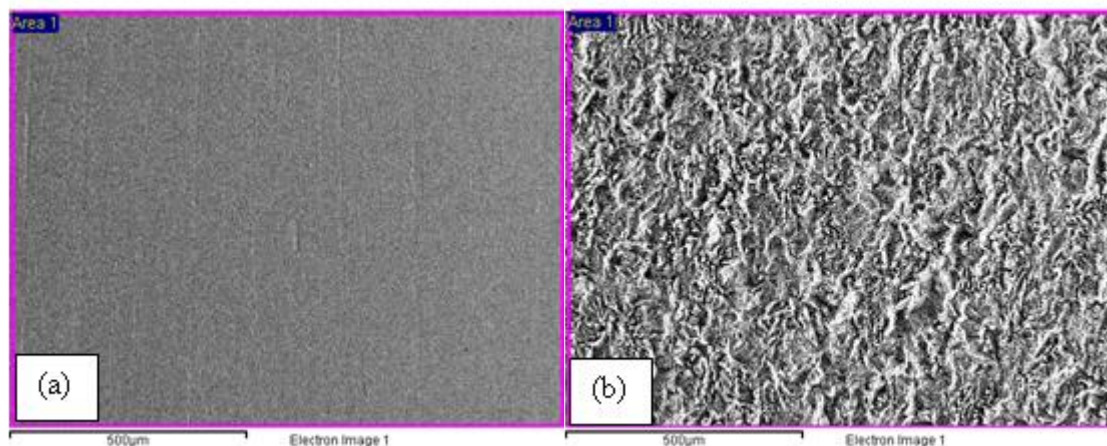
Table 5. Calculated parameters for Langmuir adsorption isotherm.

$T \text{ (K)}$	$K_{ads} \text{ (L mg}^{-1}\text{)}$	$K_{ads} \text{ (M}^{-1}\text{)}$	r^2	$\Delta G \text{ (kJ mol}^{-1}\text{)}$
303	0.0789	2.91×10^4	0.9944	-36.01
308	0.0350	1.29×10^4	0.9835	-34.52
318	7.68×10^{-3}	2.83×10^3	0.8088	-31.63
328	1.90×10^{-3}	7×10^2	0.8175	-28.82

3.3 SEM-EDX analysis

Fig. 11 (a) depicts the morphologies of polished mild steel. SEM micrographs obtained from mild steel surface after 24 hours of immersion in 1 M HCl for the untreated mild steel and treated mild steel in 60 ppm and 80 ppm extract are shown in Figs. 11 (b, c, d), respectively. Figs. 12 (a, b, c and d) represents EDX of polished mild steel, exposed to 1 M HCl, and treated mild steel in 60 ppm and 80 ppm extract, respectively.

It can be clearly observed that the mild steel surface was strongly damaged with areas of uniform corrosion where the metal is attacked more or less evenly over the entire surface. Examination on the surface morphology of treated mild steel in 60 ppm extract reveals that the metal surface is in better conditions by having smooth surfaces compared to the untreated mild steel.



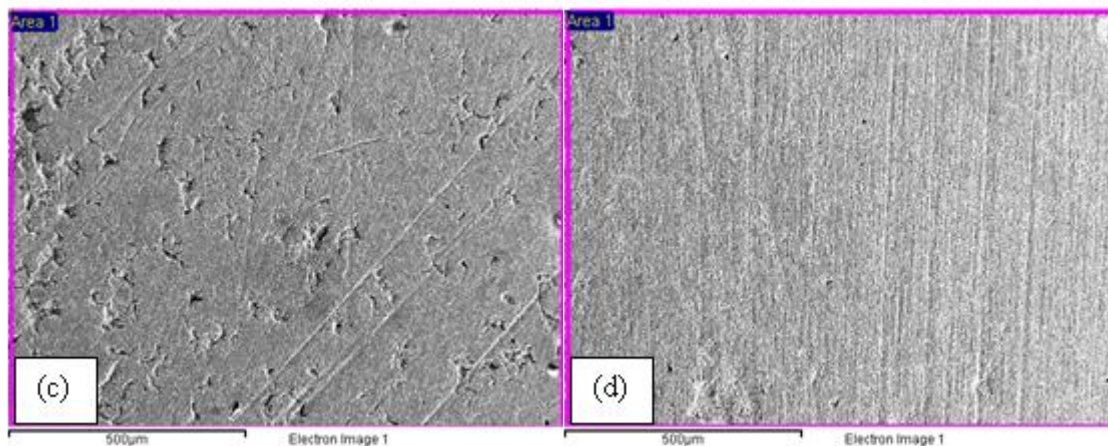
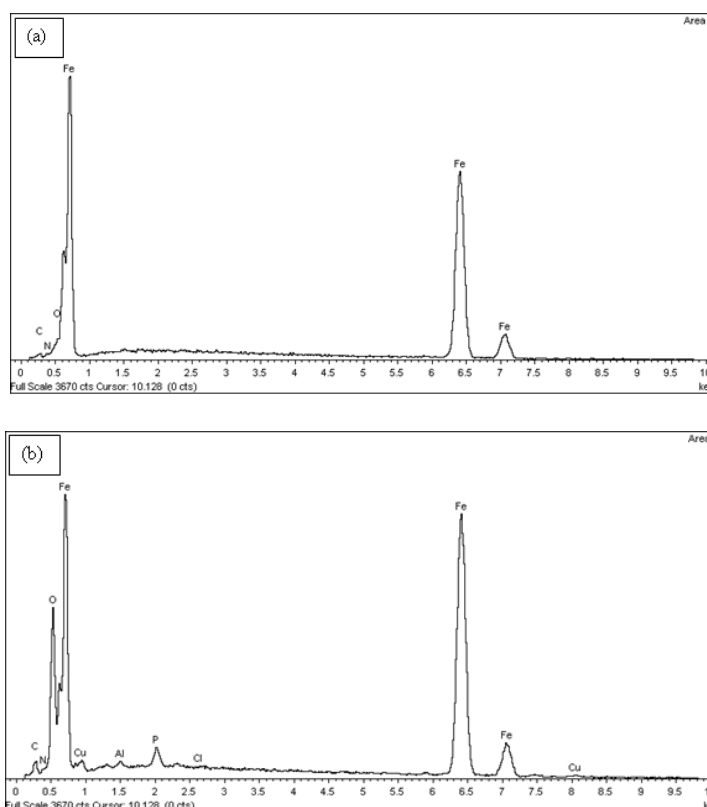


Figure 11. SEM micrographs on the surface of mild steel: (a) Polished mild steel; after 24 hours of immersion: (b) Untreated mild steel in 1 M HCl, (c) Treated mild steel in the presence of 60 ppm extract and (d) Treated mild steel in the presence of 80 ppm extract.

It can be concluded that increase in the concentration of extract will increase the smoothness of the mild steel surface as observed from Fig. 11 (d). The EDX analysis of the mild steel surface were taken at few different spots. Since the corrosive media is 1 M HCl and the extract consist mainly of carbon (C) and oxygen (O) atoms, the variation of C, chloride (Cl) and O weight percentage on the surface can be used quantitatively to explain the adsorption of extract.



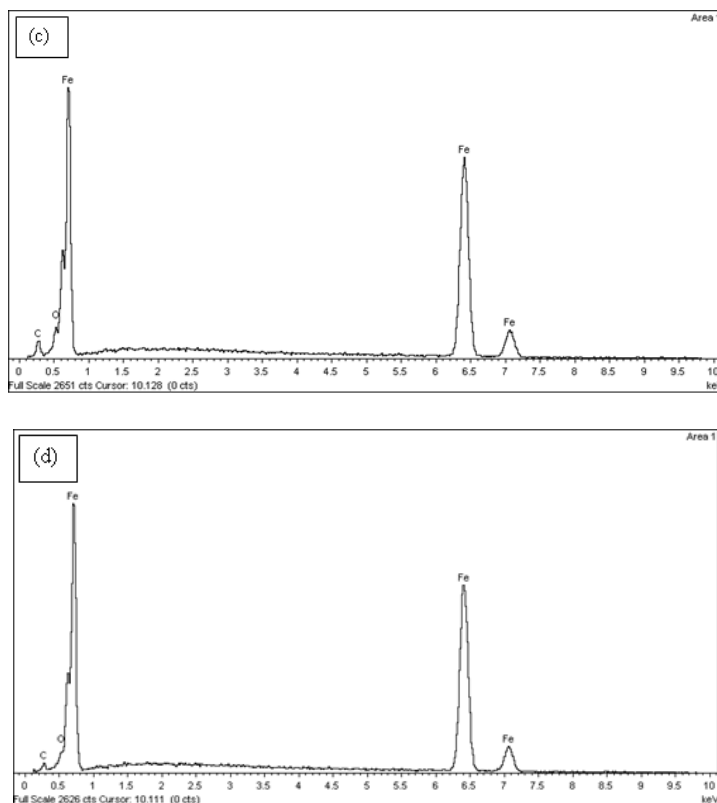


Figure 12. EDX of (a) Polished mild steel; after 24 hours of immersion: (b) Untreated mild steel in 1 M HCl, (c) Treated mild steel in the presence of 60 ppm extract and (d) Treated mild steel in the presence of 80 ppm extract.

As shown in Figs. 12, it is clear that in presence of the extract, the weight percentage (wt. %) of C increased while Cl decreased. In other words, the peak of C observed increased and the peak of Cl decreased in the presence of extract. It is also observed from Fig. 12 (b) that the O peak is high in very corrosive media in comparison to the polished and treated mild steel. Thus, it can be concluded that there is a good protective film adsorbed on the mild steel surface which is responsible for the corrosion inhibitive effect.

4. CONCLUSION

The following results can be drawn from this study:

- 1) Inhibition efficiency values increase with the inhibitor concentration but decrease with rise in temperature suggesting physisorption.
- 2) As the inhibitor concentration increased, higher activation energy, enthalpy of activation and entropy of activation were obtained. Results revealed that the inhibition is endothermic in nature and the adsorption process was more favoured at lower temperatures with larger negative standard free energy.

3) The Langmuir adsorption isotherm provide a formal description of the adsorptive behaviour of the extract on mild steel surface. The values of ΔG and K_{ads} indicate the spontaneous interaction with high adsorption ability of extract at lower temperature.

4) SEM studies reveal that the corrosion of mild steel in 1 M HCl was diminished by the addition of the extract. A smoother surface were observed.

ACKNOWLEDGEMENT

This work was carried out in the frame of research project funded by Universiti Sains Malaysia under the Research University, RU-USM-Postgraduate Research Grant Scheme, (1001/PKIMIA/834082). One of the authors (Nurul Izni Kairi) gratefully acknowledge the financial support from Yayasan Sarawak Tunku Abdul Rahman scholarship for the full sponsorship award.

References

1. P.R. Roberge, *Corrosion Engineering: Principles and Practice*, The McGraw-Hill Companies, New York (2008)
2. G.E. Badr, *Corros. Sci.* 51 (2009) 2529
3. Z. Tao, W. He, S. Wang, S. Zhang and G. Zhou, *Corros. Sci.* 60 (2012) 205
4. A. Döner and G. Kardas, *Corros. Sci.* 53 (2011) 4223
5. M.K. Pavithra, T.V. Venkatesha, M.K. Punith Kumar and H.C. Tondan, *Corros. Sci.* 60 (2012) 104
6. E.E. Oguzie, *Corros. Sci.* 50 (2008) 2993
7. H. Keleş, *Mater. Chem. Phys.* 130 (2011) 1317
8. M.A. Amin, S.S.A. El-Rehim, E.E.F. El-Sherbini and R.S. Bayoumi, *Electrochim. Acta.* 52 (2007) 3588
9. E. Bayol, A.A. Gürten, M. Dursun and K. Kayakirilmaz, *Acta Phys. Chim. Sin.* 24 (2008) 2236
10. G. Kardaş, *Mater. Sci.* 41 (2005) 337
11. F.S. de Souza and A. Spinelli, *Corros. Sci.* 51 (2009) 642
12. X. Zhou, H. Yang and F. Wang, *Electrochim. Acta.* 56 (2011) 4268
13. A.Y. El-Etre, *J. Colloid Interface Sci.* 314 (2007) 578
14. P.B. Raja and M.G. Sethuraman, *Mater. Lett.* 62 (2008) 113
15. A.O. Yüce and G. Kardaş, *Corros. Sci.* 58 (2012) 86
16. L. Valek and S. Martinez, *Mater. Lett.* 61 (2007) 148
17. M. Gopiraman, N. Selvakumaran, D. Kesavan and R. Karvembu, *Prog Org Coat.* 73 (2012) 104
18. I.B. Obot and N.O. Obi-Egbedi, *Corros. Sci.* 52 (2010) 198
19. X. Wang, H. Yang and F. Wang, *Corros. Sci.* 53 (2011) 113
20. A.R. El-Sayed, H.S. Mohran and H.M. Abd El-Lateef, *Corros. Sci.* 52 (2010) 1076
21. E.A. Noor and A.H. Al-Moubaraki, *Mater. Chem. Phys.* 110 (2008) 145
22. I.N. Levine, *Physical Chemistry*, McGraw Hill, New York (1995)
23. M.A. Amin, S.S.A. El-Rehim, E.E.F. El-Sherbini and R.S. Bayoumi, *Electrochim. Acta.* 52 (2007) 3588
24. H. Ashassi-Sorkhabi, D. Seifazadeh and M.G. Hosseini, *Corros. Sci.* 50 (2008) 3363
25. J. Ravindran, G.V. Subbaraju, M.V. Ramani, Bokyoung Sung and B.B. Aggarwal, *Biochem Pharmacol.* 79 (2010) 1658
26. H.H. Hasan, *Electrochim. Acta.* 53 (2007) 1722
27. K.W. Tan and M.J. Kassim, *Corros. Sci.* 53 (2011) 569
28. El-S.S. Abdel-Hameed, *Food Chem.* 114 (2009) 1271

29. H. Zarrok, A. Zarrouk, B. Hammouti, R. Salghi, C. Jama and F. Bentiss, *Corros. Sci.* 64 (2012) 643
30. M.M. Fares, A.K. Maayta and M.M. Al-Qudah, *Corros. Sci.* 60 (2012) 112
31. M. Behpour, S.M. Ghoreishi, M. Khayatkashani and N. Soltani, *Mater. Chem. Phys.* 131 (2012) 621
32. A.K. Singh, S.K. Shukla, M. Singh and M.A. Quraishi, *Mater. Chem. Phys.* 129 (2011) 68
33. Z. Tao, W. He, S. Wang, S. Zhang and G. Zhou, *Corros. Sci.* 60 (2012) 205
34. S. Garai, P. Jaisankar, J.K. Singh and A. Elango, *Corros. Sci.* 60 (2012) 193
35. M.R. Singh, K. Bhrara and G. Singh, *Port. Electrochim. Acta.* 26 (2008) 479
36. S.A. Umoren, Y. Li and F.H. Wang, *Corros. Sci.* 52 (2010) 1777
37. J. Zhang, W.W. Song, D.L. Shi, L.W. Niu, C.J. Li and M. Du, *Prog. Org. Coat.* 75 (2012) 284
38. E.S. Meresht, T.S. Farahani and J. Neshati, *Corros. Sci.* 54 (2012) 36
39. S. Hong, W. Chen, H.Q. Luo and N.B. Li, *Corros. Sci.* 57 (2012) 270
40. N.O. Obi-Egbedi and I.B. Obot, *Corros. Sci.* 53 (2011) 263
41. S.T. Keera and M.A. Deyab, *Colloids and Surfaces.* 266 (2005) 129
42. E.E. Ebenso, *Mater. Chem. Phys.* 79 (2003) 58
43. A.K. Singh, S.K. Shukla, M. Singh and M.A. Quraishi, *Mater. Chem. Phys.* 129 (2011) 68
44. M. Kissi, M. Bouklah, B. Hammouti and M. Benkaddour, *Appl. Surf. Sci.* 252 (2006) 4190
45. E.E. Foad El-Sherbini, S.M. Abdel Wahaab and M. Deyab, *Mater. Chem. Phys.* 89 (2005) 183
46. X. Zhou, H. Yang and F. Wang, *Electrochim. Acta.* 56 (2011) 4268
47. X. Li, S. Deng and H. Fu, *Prog. Org. Coat.* 67 (2010) 420
48. F. Zhang, Y. Tang, Z. Cso, W. Jing, Z. Wu and Y. Chen, *Corros. Sci.* 61 (2012) 1
49. A.K. Singh and M.A. Quraishi, *Corros. Sci.* 53 (2011) 1288
50. A.K. Singh, S.K. Shukla, M.A. Quraishi and E.E. Ebenso, *J. Taiwan Inst. Chem. E.* 43 (2012) 463
51. W.H. Li, Q. He, S.T. Zhang, C.L. Pei and B.R. Hou, *J. Appl. Electrochem.* 38 (2008) 289
52. E. Bensajjay, S. Alehyen, M. El Achouri and S. Kertit, *Anti-Corros. Meth. Mater.* 50 (2003) 402
53. X. Li, S. Deng and H. Fu, *Corros. Sci.* 51 (2009) 1344